

Electronic Supporting information (ESI)

Small-molecule ligands strongly affect the Förster resonance energy transfer between quantum dot and fluorescent protein

Yue Zhang, Haiyan Zhang, Jeff Hollins, Michael E. Webb and Dejian Zhou*

School of Chemistry and Astbury Centre for Structural Molecular Biology, University of Leeds, Leeds LS2 9JT, United Kingdom. Fax: +44 113 3436565; Tel: +44 113 3436230; E-mail: d.zhou@leeds.ac.uk.

Quantum yield

The method for quantum yield determination used here is the comparative method, which involves the use of a standard sample of known quantum yield value. In this regard, Rhodamine 6G (in ethanol under 480 nm excitation) was used as the standard whose quantum yield is 0.95. The QD quantum yields were calculated by the equation:

$$Y_u = Y_s \cdot (F_u/F_s) \cdot (A_s/A_u)$$

Where Y_u , F_u and A_u are the quantum yield (QY), integrated fluorescence intensity and absorbance at 480 nm of the QD sample, and Y_s , F_s , and A_s are the quantum yield, integrated fluorescence intensity and absorbance at 480 nm of the standard (Rhodamine 6G).

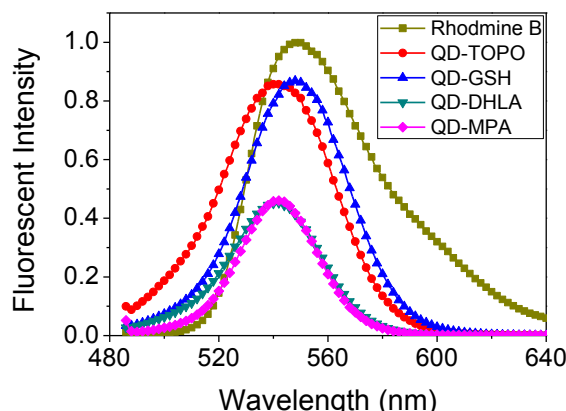


Fig. S1 The relative fluorescent spectra of the QDs (all of the same concentration).

Time-based titration experiments

As the representatives of Group I and II respectively, titrations of the two QD-FP systems (QD(MPA)-FP and QD(GSH)-FP) were investigated here using time base scan program (Fig. S2).

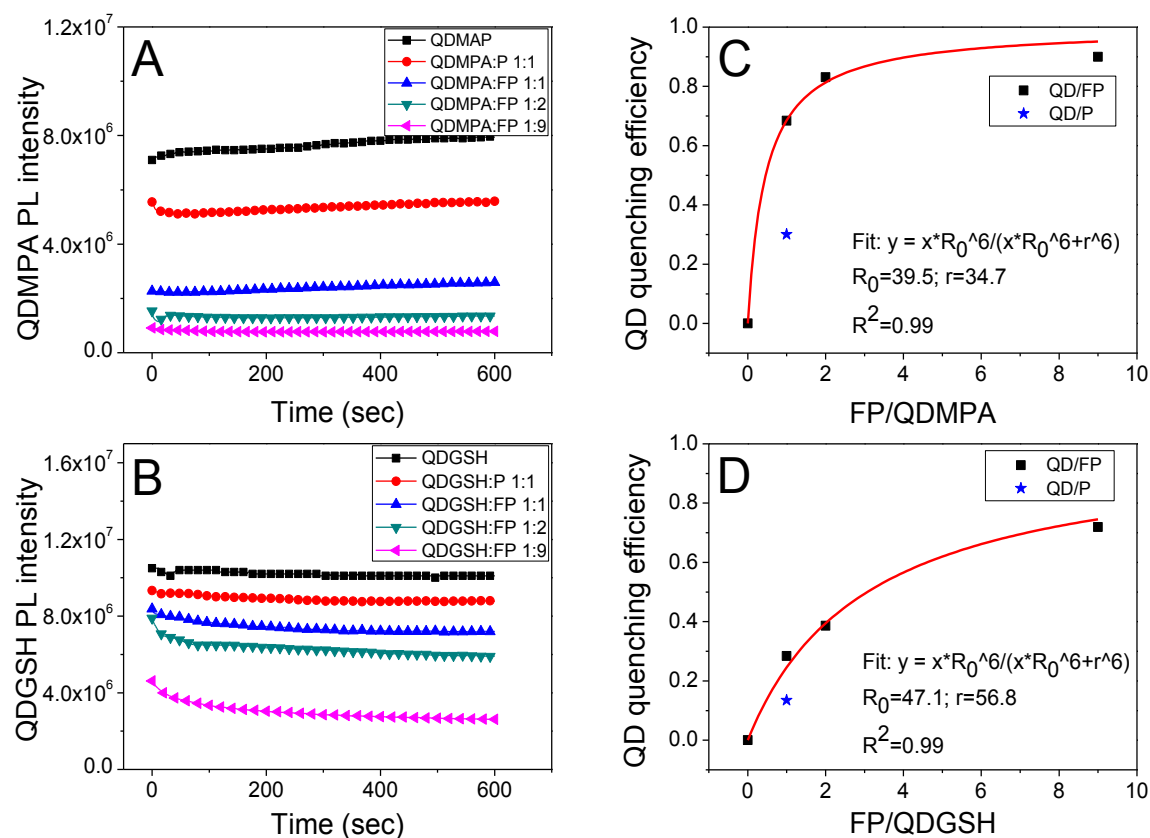


Fig. S2. Time based fluorescent intensity scans and the corresponding QD quenching efficiencies. Time based QD PL intensity of QD(MPA)-FP (**A**) and QD(GSH)-FP (**B**) conjugates. Plots of the QD quenching as a function of the FP-to-QD ratio for QD(MPA)-FP (**C**) and QD(GSH)-FP conjugates (**D**).

The concentration of the QDs was maintained at 40 nM while the ratio of FP/P to QD was changed. The required amount of H₂O, 10 × PBS and FP were first added into a cuvette placed in the fluorimeter, and then the time based scan program was triggered immediately once the required amount of QD solution was added in.

The excitation wavelength (425 nm) was the same as that used in emission scan method. While the emission wavelengths, where the intensity data were collected,

were selected to be 538 nm for QD(MPA) and 545 nm for QD(GSH), corresponding to the maximum emission peaks of the two QDs. Both the excitation and emission band-path are 5 nm.

These studies on QD-FP titrations using time based scan method show that the calculated distances between QD and FP are 34.7 Å for QD(MPA)-FP and 56.8 Å for QD(GSH)-FP, which are consistent with the QD-FP titrations results (36.0 Å for QD(MPA)-FP and 61.0 Å for QD(GSH)-FP) obtained by emission scan method. For the QD-P (1:1) system, the engineered non-fluorescent protein P with His₆-tag could also quench the QD PL intensity. The quenching effect is stronger for the QD(MPA)-P compared to the QD(GSH)-P system with quenching efficiencies of 0.30 and 0.14 respectively.

Gel-filtration chromatography

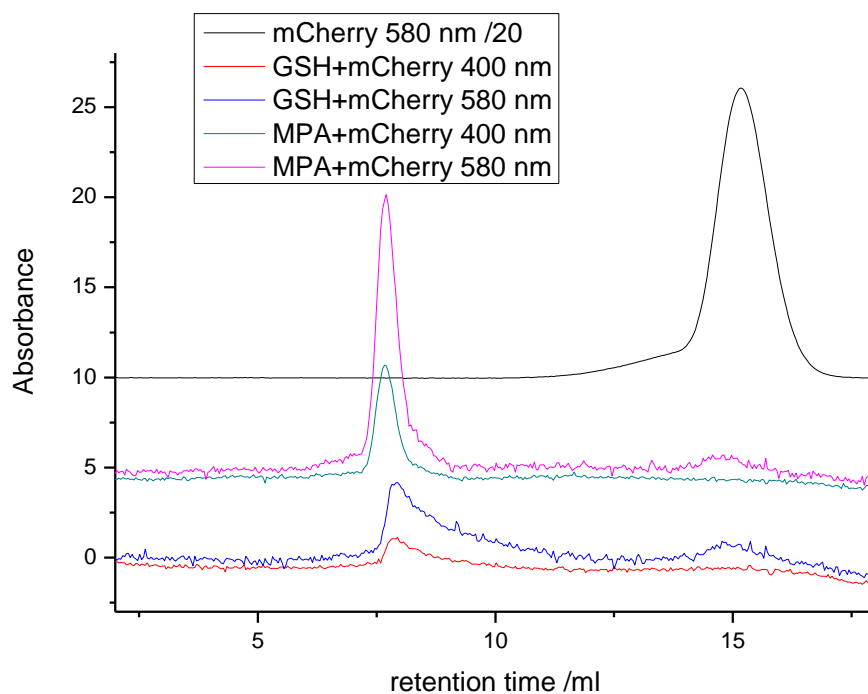


Fig. S3 gel-filtration chromatography for QD(MPA), QD(GSH) and FP.

TEM images

To examine whether the size of the core/shell QDs has changed after the ligand exchange, *i.e.* the original TOPO ligands were substituted by water-soluble ligands, TEM images have been taken (see Fig.S2) on MPA and GSH capped core/shell QDs.

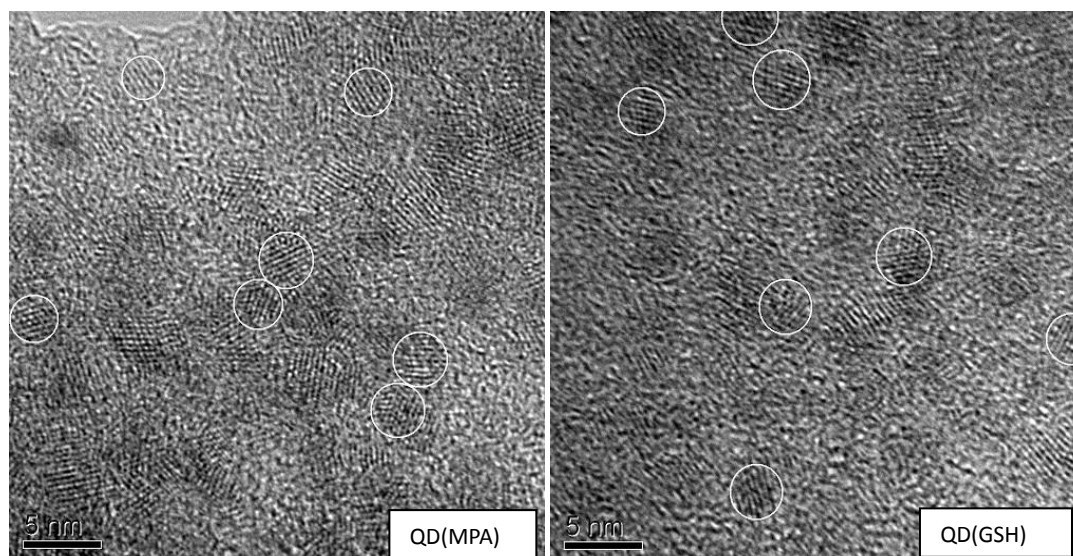


Fig. S4 Representative TEM images for QD(MPA) and QD(GSH).

It is possible to see QD particle crystal lattice, suggesting these QDs are highly crystalline, but the particle borders could not be identified clearly. A few white circles drawn on each QD crystals were used to indicate the rough diameters of the QD particles, and these gave a rough QD diameter of about 3.4 nm, consistent with the product description from the manufacture (*e.g.* crystal diameter ~ 3.4 nm).